

Inhibitor Effect of *Anthocleista djalensis* Extract on the Corrosion of Concrete Steel Reinforcement

Gengfang Xie*, Liu Wei

School of architecture, Chang'an University, Xi'an, Shaanxi, 710064, P.R. China

*E-mail: gengfangxie_hi@163.com

Received: 7 February 2018 / Accepted: 21 March 2018 / Published: 10 May 2018

In the present study, the anticorrosion behaviour of the leaf-extract admixture of *Anthocleista djalensis* (*A. djalensis*) on steel-reinforced concrete immersed in an HCl solution (as an aggressive medium) was investigated using electrochemical methods. Monitoring-related parameters included the corrosion rate, corrosion potential, and corrosion current. The performance of this novel eco-friendly corrosion inhibitor was investigated at various temperatures (25–60 °C) at various concentrations (0.1 to 0.4 g/L).

Keywords: Corrosion of steel reinforcement; Inhibitor; Inhibition efficiency; *Anthocleista djalensis*

1. INTRODUCTION

The corrosion of steel reinforcements in concrete has raised significant concerns due to its impact on the integrity of infrastructure and building structures. Due to its ease of manufacturing, low cost, and high versatility, steel-reinforced concrete still occupies a dominating position worldwide [1-3]. The steel reinforcement of concrete is generally protected using a thin layer of oxide film in pH > 12 concrete pores [4-8]. Unfortunately, this passive thin oxide layer can be damaged by low pH brought about by aggressive acidifying chemicals in the environment. Under these conditions, concrete steel-rebar is prone to corrosion degradation. There are several sources of such acidifying chemicals. For instance, HCl may be derived from wastewater in industrial environments [9-18]. Concrete can be attacked by HCl through the formation of an electrochemical cell of steel-reinforcement corrosion along with expansive volume products; if left unchecked, this cell would lead to the collapse of the steel-reinforced concrete structure [19-23].

Many previous reports proposed the effective and facile mitigation of steel-reinforced concrete corrosion degradation in an acidic HCl environment using corrosion inhibitors as admixtures in the

concrete [24-27]. Among these, chromate- and nitrite-based compounds have been found to effectively inhibit steel-rebar corrosion. They also have certain disadvantages, such as toxicity, which poses hazards to the environment and limits their application [28-32]. Additionally, these synthetic and inorganic chemical inhibitors are expensive and difficult to synthesize [2, 33, 34]. Therefore, it is necessary to develop green, cost-effective, and easily available substitutes to solve problems related to steel-reinforced concrete corrosion degradation problems in an acidic HCl environment.

Extracts from various parts (root bark, stem bark, and leaf) of *Anthocleista djalonenensis* (*A. djalonenensis*) have been found to show both *in vivo* and *in vitro* capabilities for healing a wide range of diseases [35, 36]. In addition, aluminium corrosion inhibition under an HCl environment has been studied using the extract from the stem bark of *A. djalonenensis*. Notably, the toxicity of the *A. djalonenensis* leaf extract has been found to be lower than that of the stem bark [37]. Additionally, all test animals treated with the *A. djalonenensis* leaf extract (5000 mg/kg) survived, whereas all test animals treated with the stem bark extract (2500 mg/kg) died [36]. In addition, the inhibition of the leaf extract of *A. djalonenensis* on the corrosion of steel reinforcement in concrete immersed in a chloride-contaminated solution has also been reported [2]. Fourier transfer infrared (FTIR) results showed that the test leaf extract consisted of aromatic compounds that were potent with π -electrons, which could interact with the vacant *d*-orbital of Fe in the steel rebar in concrete [2]. It was also found that *A. djalonenensis* contains mixed compounds, including tannins, saponins, phlobatanins, flavonoids, and alkaloids. These constituents have been reported to exhibit a remarkable inhibitory effect on mild steel in acidic chloride (HCl) solution [38]. To date, no study has reported the inhibitory effect of the leaf extract of *A. djalonenensis* on the corrosion of steel reinforcement in a concrete slab immersed in a HCl solution. Therefore, this paper studies this anticorrosion performance in an acidic environment by simulating the industrial/microbial setting. Methods for the electrochemical monitoring of steel reinforcement corrosion were employed and analysed to detail the anticorrosion performance of various concentrations of *A. djalonenensis* leaf-extract admixture on steel-reinforced concrete samples.

2. EXPERIMENTS

2.1. Synthesis of the leaf extracts of *Anthocleista djalonenensis*

The leaf extracts used in this study were prepared according to existing literature [39, 40]. Samples of *Anthocleista djalonenensis* were obtained from a farm in Aba North, Abia State. After complete washing to remove dirt, the collected leaves were left to dry in air. The powdered form was generated after pulverizing these leaves. To prepare the stock solution, 10 g of the prepared powder was refluxed in HCl solution (240 ml; 1.0 M), followed by filtration of the resulting mixture. With excess 1.0 M HCl as the solvent, various concentrations were prepared from the prepared stock solution (0.1 - 0.6 g/L). The preparation was performed at 333 K and at ambient temperature. FT-IR spectra were recorded on a Perkin Elmer 1750 FTIR Spectrophotometer.

2.2. Preparation of steel reinforced concrete samples

The test steel reinforcement was 12 mm in diameter. The elemental composition of this deformed steel rebar was as follows: 0.273% C, 0.780% Mn, 0.403% Si, 0.240% Cu, 0.142% Cr, 0.109% Ni, 0.039% P, 0.037% S, 0.016% Mo, 0.0086% Co, 0.0083% Nb, 0.0063% Sn, 0.0037% Ce, 0.0032% V, and the balance was Fe. For corrosion measurements, the rebar was cut into steel rods of 190 mm. For all of these steel rods, surfaces were first prepared by grinding using abrasive paper of various grades. Samples were pickled in H₂SO₄ (10%), rinsed and cleaned in an ultrasonic cleaner. After degreasing in acetone, they were dried under a warm air stream. Finally, 150 mm of each steel rod was centrally embedded into a concrete slab (100 × 100 × 200 mm).

2.3. Electrochemical experiments

To simulate a real microbial/industrial environment, we immersed the steel-reinforced concrete samples partially and longitudinally in plastic bowls containing an HCl solution (1 M) using standard procedures. The concrete was immersed in the HCl test solution so that the steel protruding from the concrete was just above the solution level but did not touch it. To maintain the corrosive environment, we replenished the test solution every three weeks. Electrochemical impedance spectroscopy (EIS) and polarization techniques (Autolab potentiostat/galvanostat) were performed to study the inhibition effects of *A. djalonensis* on the surface of the steel in the 1 M HCl solution at various temperatures (25, 40, 50 and 60 °C) before and after the addition *A. djalonensis* (0.1, 0.2, 0.3 and 0.4 g/L). The experiments were performed with open circuit potential (OCP) after immersion for 120 min, where the electrode reached a steady state. In addition, potentiodynamic experiments were initiated in the cathodic to the anodic direction at ± 250 mV near OCP (scan rate, 1.0 mV/s). The parameters for the EIS measurements were described as follows: frequency range, 100 kHz to 10 mHz; peak to zero amplitude, ± 10 mV. Data analysis was performed using Nova (ver 1.7) software.

3. RESULTS AND DISCUSSION

The extract of *A. djalonensis* leaf was characterized by FTIR. A broad band between 3457 cm⁻¹ is due to the N–H stretching vibration of the NH₂ and OH group, and the overlapping of the stretching vibration is attributed to water and the *A. djalonensis* leaf extract. The band at 1634 cm⁻¹ corresponds to amide CO stretching, and a peak at 2085 cm⁻¹ can be assigned to the alkyne group present in the phytoconstituents of the extract. The observed peaks at 1111 cm⁻¹ denote –C–OC– linkages or –C–O–bonds. The observed peaks are primarily attributed to flavanoids and terpenoids that are excessively present in the plant extract [41, 42]. On the other hand, the prepared extract sample shows a wide, strong peak with a maximum intensity at 557 cm⁻¹. The results are in good agreement with those found in the literature [43].

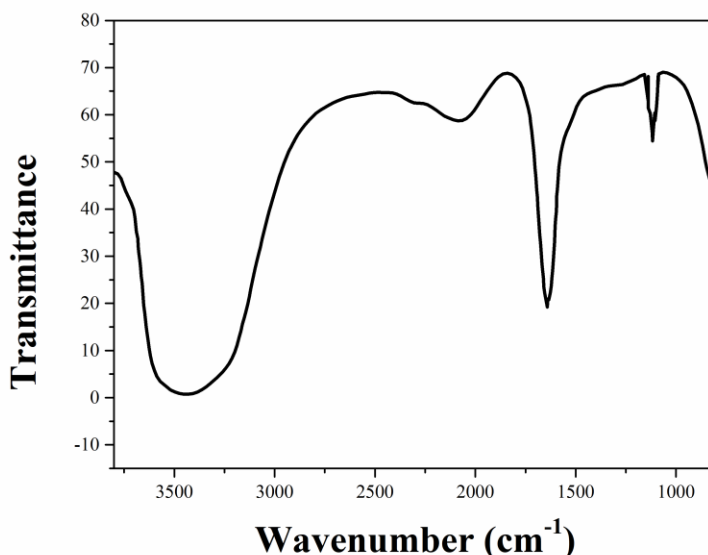


Figure 1. FTIR spectrum of *A. djalonenensis* leaf extract.

Fig. 2 shows both the cathodic and anodic polarization curves for the carbon steel samples immersed in HCl solution (1 M) before and after the addition of *A. djalonenensis* at varying concentrations (0.1, 0.2, 0.3 and 0.4 g/L) and varying temperatures (25, 40, 50 and 60 °C). Table 1 shows the corrosion current density (I_{corr}), corrosion potential (E_{corr}), cathodic Tafel slope (β_c) and inhibition efficiency (IE %). It was observed that temperature could affect inhibition efficiency; 40 °C showed the highest inhibition efficiency among all tested temperatures. Moreover, the increasing concentration of the *A. djalonenensis* leaf extract could result high inhibition efficiency, in agreement with other plant extracts [44-46]. It is also noteworthy that in the anodic branches of the curves, we did not observe the linear Tafel region. Therefore, the anodic Tafel slopes (β_a) could not be obtained using an interpolation method, along with another more significant parameter, the corrosion current density (I_{corr}). To solve this problem, the interpolation of the cathodic asymptote with the line crossing the E_{corr} has been described as I_{corr} .

Table 1. Electrochemical polarization parameters for the carbon steel before and after adding *A. djalonenensis* at varying concentrations (0.1, 0.2, 0.3 and 0.4 g/L) at varying temperatures.

Sample	E_{corr} (mV)	I_{corr} (μ A/ cm^2)	β_c (V/dec)	β_a (mV/dec)	IE%
25 °C					
Blank	-460	513.2	0.10	0.08	0
0.1 g/L	-457	420.4	0.09	0.07	18.08
0.2 g/L	-468	308.1	0.09	0.05	39.96
0.3 g/L	-452	220.7	0.09	0.06	56.99
0.4 g/L	-447	99.5	0.09	0.05	80.61
40 °C					
Blank	-477	533.6	0.11	0.06	0
0.1 g/L	-487	445.2	0.10	0.05	16.57
0.2 g/L	-476	289.6	0.10	0.05	45.73

0.3 g/L	-458	188.4	0.09	0.04	64.69
0.4 g/L	-479	77.5	0.10	0.04	85.78
50 °C					
Blank	-481	566.6	0.10	0.06	0
0.1 g/L	-476	472.4	0.11	0.08	16.63
0.2 g/L	-478	305.6	0.10	0.08	46.06
0.3 g/L	-476	215.5	0.10	0.07	61.97
0.4 g/L	-477	110.0	0.11	0.06	80.59
60 °C					
Blank	-480	580.5	0.09	0.07	0
0.1 g/L	-475	496.0	0.10	0.08	14.56
0.2 g/L	-475	432.5	0.11	0.08	25.50
0.3 g/L	-472	398.6	0.11	0.09	31.34
0.4 g/L	-473	200.4	0.12	0.09	65.49

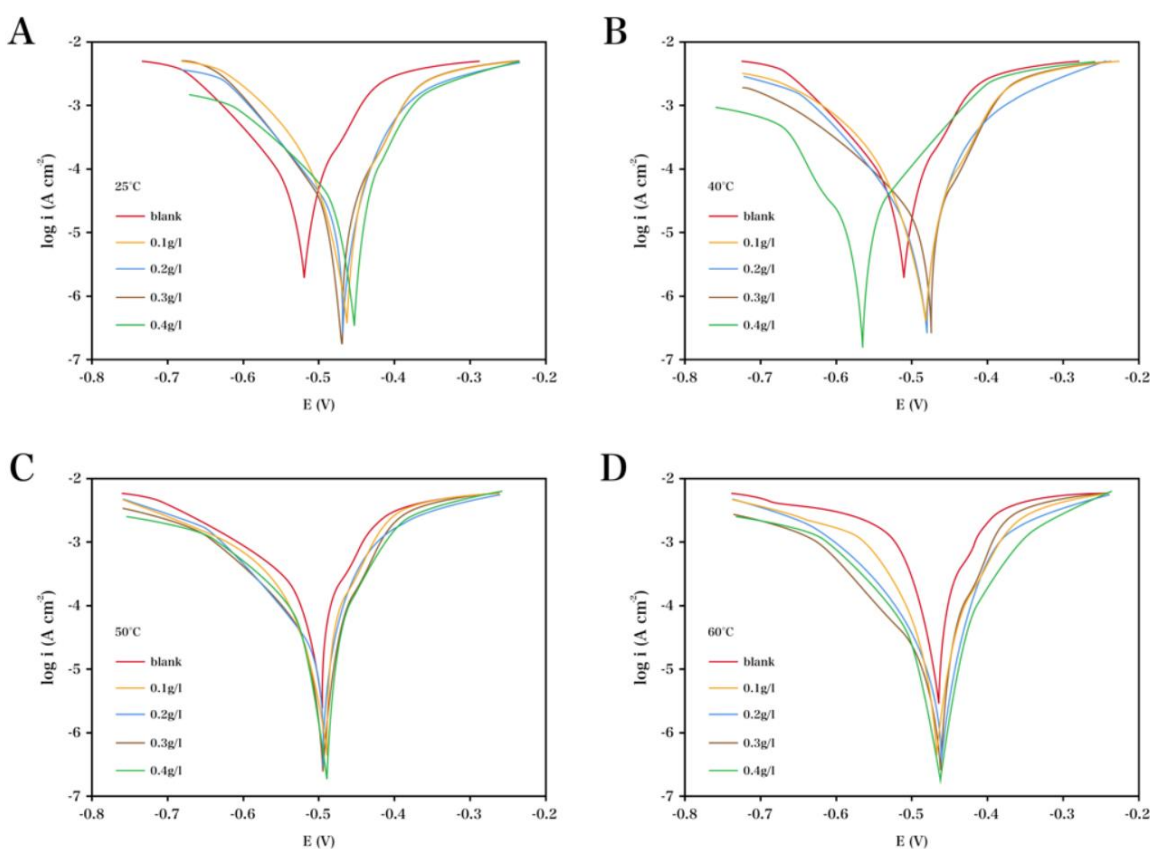


Figure 2. Polarization plots of the samples immersed in HCl solution (1 M) before and after adding varying concentrations of *A. djalensis* at varying temperatures.

Upon the addition of *A. djalensis*, even at a low level, into the 1 M HCl solution, the cathodic and anodic branches both shifted to lower current densities, and corrosion potential slightly shifted towards less negative values (Fig. 2A). Therefore, as the concentration of *A. djalensis* increased, a decrease in corrosion current density was observed as well as elevated inhibition efficiency. Additionally, the cathodic Tafel slope sharply decreased, together with a small corrosion

potential increase to less negative values, in the case of increased *A. djalonenensis* concentration. This means that the effect of *A. djalonenensis* on the shape of the anodic branch is more significant than that of the cathodic branch. These results confirm the predominant role of *A. djalonenensis* (a mixed-type inhibitor) in anodic reactions. As shown in Fig. 2B-D, measurements were performed using carbon steel in HCl solutions (1 M) before and after the addition of *A. djalonenensis* at various temperatures (40, 50 and 60 °C). Upon the increase in temperature, we observed an increasing tendency for both the corrosion current density and the corrosion rate but a decreasing tendency for the corrosion inhibition efficiency. This results from the carbon steel oxidation rate increasing in the HCl solution after the temperature increase [47]. It also confirms that the impedance of the inhibited substrate increases with the concentration of extract [48]. However, even at 60 °C, *A. djalonenensis* still exhibited a high inhibition efficiency of 84%, which suggests that it is highly inhibitory in HCl solution (1 M), even at high temperatures.

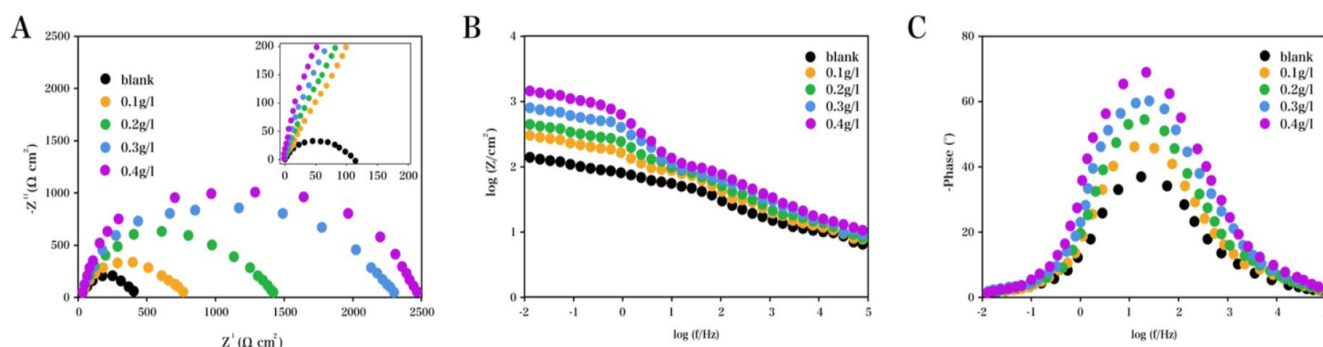


Figure 3. (A) Nyquist and (B,C) Bode plots recorded for the samples immersed in HCl solution (1 M) before and after adding varying concentrations of *A. djalonenensis* at 25 °C.

Table 2. Element value of a circuit equivalent to fit the impedance spectra in Figure 3 and the values of the corrosion efficiency.

Sample	R_s (Ω/cm^2)	R_{ct} (Ω/cm^2)	C_{dl} ($\mu\text{F}/\text{CM}^2$)	IE(%)
Blank	8.77	88.96	15.24	0
0.1 g/L	7.05	110.56	5.02	19.54
0.2 g/L	7.03	131.93	5.77	32.57
0.3 g/L	6.48	220.52	6.98	59.66
0.4 g/L	6.84	495.32	10.51	82.04

After immersion for 120 min, the carbon steel corrosion performance in 1 M HCl solution before and after *A. djalonenensis* was studied at various temperatures using the EIS method. Figs. 2-5 show the Nyquist and Bode plots. The Nyquist plots are obviously not semicircles, which suggests that the surface is inhomogeneous. On the bare sample and others immersed in 1 M HCl solutions containing *A. djalonenensis* (0.1 and 0.2 g/L), the electrochemical reactions were studied using a one-time constant electrical circuit. This reveals the electron transfer-controlled property of these electrochemical reactions on the samples. However, for samples immersed in 1 M HCl solutions

containing *A. djalonensis* (0.3 and 0.4 g/L), the corresponding Nyquist and Bode plots were better fitted with a two-time constant electrical mode. As seen from Tables 2-5, R_{ct} increases with the assembly time, and C_{dl} decreases with extract concentration. The adsorption extract increases the thickness of the double layer capacitance, which can increase the R_{ct} and decrease the corrosion reaction rate [49, 50].

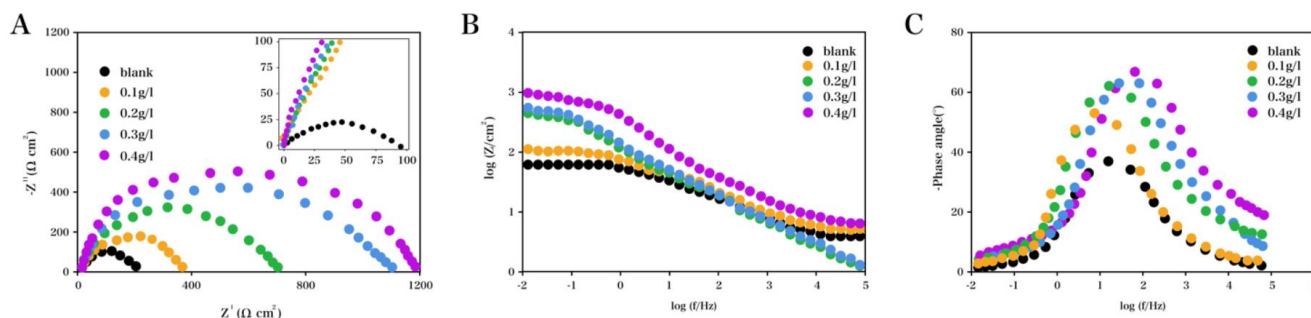


Figure 4. (A) Nyquist and (B,C) Bode plots recorded for the samples immersed in HCl solution (1 M) before and after adding varying concentrations of *A. djalonensis* at 40 °C.

Table 3. Element value of a circuit equivalent to fit the impedance spectra in Figure 4 and the values of the corrosion efficiency.

Sample	R_s (Ω/cm^2)	R_{ct} (Ω/cm^2)	C_{dl} ($\mu F/CM^2$)	IE(%)
Blank	8.54	90.59	14.25	0
0.1 g/L	7.26	107.21	7.71	15.50
0.2 g/L	7.11	156.40	5.23	42.08
0.3 g/L	6.59	298.97	6.99	69.03
0.4 g/L	7.03	788.42	11.01	88.51

R_{ct} increased with the inhibitor concentration increase, since the inhibitor molecules were adsorbed onto the anodic/cathodic sites of the metal surface. The overlapped two time constants related to R_{ct} and R_f —for the samples immersed in 1 M HCl solutions containing *A. djalonensis* (0.3 and 0.4 g/L)—were separated by fitting. The results showed that $R_f \ll R_{ct}$, which suggested that a thick film was not generated by the inhibitors after their adsorption onto the steel surface and that the electrochemical reactions at a high-level concentration of inhibitors remained controlled by electron transfer resistance. Access of aggressive species to the metal surface was blocked after the inhibitors were adsorbed onto the active sites of the steel surface [51]. As the inhibitor concentration was elevated, a reduction in C_{dl} was observed, suggesting that the concentration increase enhanced the adsorption of inhibitor molecules onto the surface of steel. Additionally, as the concentration increased, an increase was found in the homogeneity parameter (n), which suggested that the surface became less heterogeneous and less rough [52]. When using the sample immersed in the solution containing 0.4 g/L inhibitor, the maximal inhibition efficiency was obtained (93%). This behaviour confirmed the results obtained from the polarization measurements, which indicates that the reduction process is controlled by diffusion of oxygen from the bulk solution to the surface [53]. The results

showed that the breakpoint frequency (f_b) decreased with the increase in inhibitor concentration, which suggested that an increasing number of inhibitor molecules were adsorbed on the surface of steel. When using the samples containing 0.3 and 0.4 g/L *A. djalonenisis*, the capacitive region was observed over a wider frequency range, possibly due to the higher number of adsorbed inhibitors on the steel surface. The phase angel of the phase plot was elevated with increased inhibitor concentration, most obviously in the case of the 0.3 and 0.4 g/L inhibitors [54].

The inhibitor showed a *ca.* 9% decrease in inhibition efficiency with the electrolyte temperature increase. The inhibition efficiency decrease was primarily due to two factors: some adsorbed inhibitors were desorbed from the steel surface, and the dissolution rate of metal was increased.

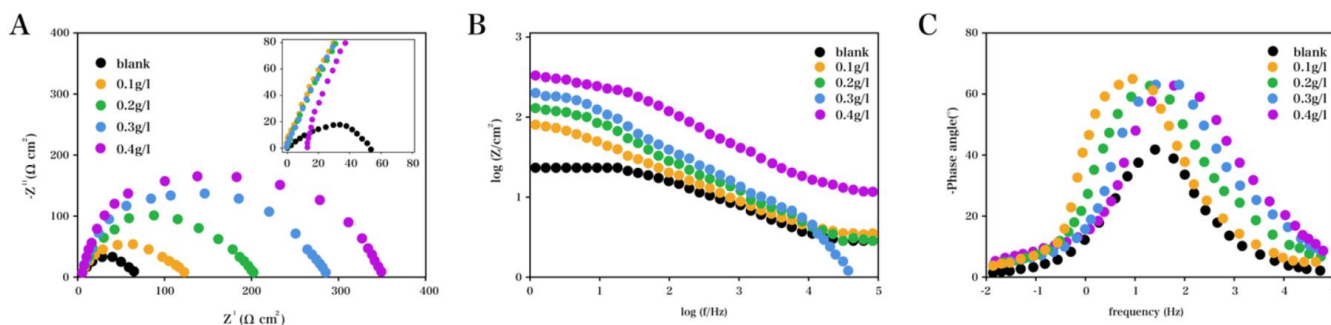


Figure 5. (A) Nyquist and (B,C) Bode plots recorded for the samples immersed in 1 M HCl solution before and after adding varying concentrations of *A. djalonenisis* at 50 °C.

Table 4. Element value of a circuit equivalent to fit the impedance spectra in Figure 5 and the values of the corrosion efficiency.

Sample	R_s (Ω/cm^2)	R_{ct} (Ω/cm^2)	C_{dl} ($\mu F/CM^2$)	IE(%)
Blank	7.76	65.08	10.54	0
0.1 g/L	4.51	78.22	7.78	16.80
0.2 g/L	3.27	105.65	5.52	38.41
0.3 g/L	2.51	173.55	5.12	62.54
0.4 g/L	3.35	306.98	8.01	78.80

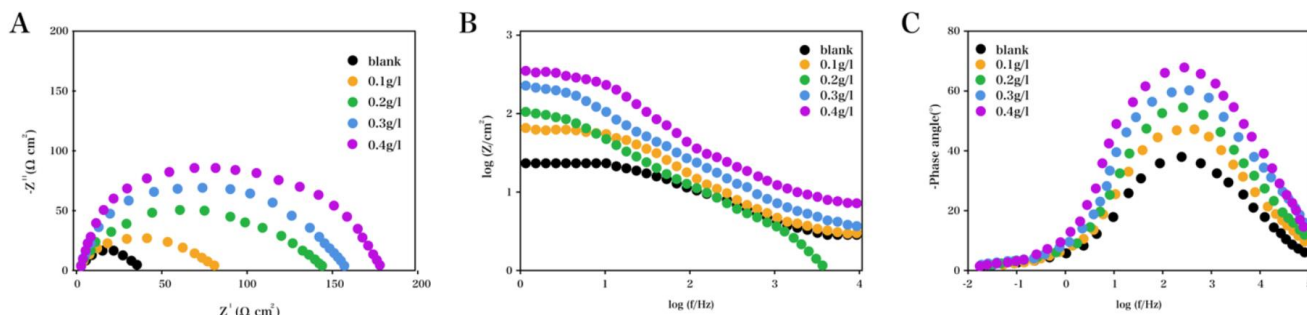


Figure 6. (A) Nyquist and (B,C) Bode plots recorded for the samples immersed in 1 M HCl solution before and after adding varying concentrations of *A. djalonenisis* at 60 °C.

Table 5. Element value of a circuit equivalent to fit the impedance spectra in Figure 6 and the values of the corrosion efficiency.

Sample	R_s (Ω/cm^2)	R_{ct} (Ω/cm^2)	C_{dl} ($\mu\text{F}/\text{CM}^2$)	IE(%)
Blank	9.60	40.02	10.24	0
0.1 g/L	5.54	44.74	6.51	10.54
0.2 g/L	3.21	52.96	5.05	24.44
0.3 g/L	1.19	62.93	4.03	36.51
0.4 g/L	2.56	80.86	7.75	50.51

The presence of heteroatoms due to *A. djalonenensis*, i.e., N and O, may be derived from hydrocarbons and aromatic rings from other phytoconstituents in the extracts. On the surface of the steel, there are active cathodic and anodic sites that can lead to serious steel dissolution through contact with the aggressive species. The surface of carbon steel can block the adsorption of extract inhibitor against charge and mass transfer, leading to hindrance of the corrosion process. In general, there are two modes of adsorption. First, the neutral compounds of the extract components show adsorption via a chemisorption mechanism, where the electrons between N or O atom and Fe can be shared; the water molecules can be displaced from the metal surface. For the components of the extract inhibitor, adsorption can be realized through π electrons in the fused benzene rings and the vacant D-orbital of iron. Regardless of the number of components present in the system, the adsorption equilibrium of pure components is an essential ingredient for understanding how many components can be accommodated by a solid adsorbent [55]. However, the protonated components of the extract inhibitor show a physical adsorption via electrostatic interactions between the adsorbed chloride ions and the cations. The extracts' physisorption onto the carbon steel surface was evidenced by the thermodynamic results. The following chemical reactions are proposed for the steel and ion corrosion in HCl solution. The potentiodynamic polarization results show that *A. djalonenensis* operates via a mixed inhibitory mechanism. In the HCl solution, some components of *A. djalonenensis* can be protonated and adsorbed via the π electrons of the aromatic ring onto the cathodic sites of the carbon steel surface. The anodic dissolution of the carbon steel can be inhibited through the interaction between the vacant D-orbital of iron and the lone pair of electrons of the heteroatoms (N, O).

Table 6. Inhibition performance comparison of different inhibitors prepared by plant.

Plant extract	Specimen	IE(%)	Reference
<i>Mansoa alliacea</i>	Zinc	87.72	[56]
<i>Annona squamosa</i>	C38 steel	95.21	[57]
<i>Isertia coccinea</i>	Mild steel	75.60	[58]
<i>Oxandra asbeckii</i>	C38 steel	85.06	[59]
<i>Argemone mexicana</i>	Mild steel	90.77	[60]
<i>Justicia gendarussa</i>	Steel carbon	77.90	[38]
<i>Anthocleista Djalonenensis</i>	Steel carbon	85.78	This work

These results confirmed the mixed inhibitory mechanism of *A. djalonenensis* for the carbon steel surface in HCl solution (1 M). Table 6 compares various plant-based inhibitors; it can be seen that the proposed *A. djalonenensis* showed comparable performance.

4. CONCLUSIONS

The present report studied the electrochemical behaviour of *A. djalonenensis* leaf extract on the corrosion of concrete steel reinforcement. *A. djalonenensis* showed desirable inhibitory effects on carbon steel corrosion over a temperature range of 25 to 60 °C. Polarization results confirmed *A. djalonenensis* as a mixed-type inhibitor. Additionally, impedance experimental results exhibited an increase in electron transfer resistance with increased *A. djalonenensis* concentration.

References

1. S.A. Asipita, M. Ismail, M.Z.A. Majid, Z.A. Majid, C.S. Abdullah and J. Mirza, *Journal of Cleaner Production*, 67 (2014) 139.
2. J.O. Okeniyi, C.A. Loto and A.P.I. Popoola, *Transactions of the Indian Institute of Metals*, 67 (2014) 959.
3. F. Biondini, E. Camnasio and A. Titi, *Earthquake Engineering & Structural Dynamics*, 44 (2015) 2445.
4. Y. Liu, Y. Song, J. Keller, P. Bond and G. Jiang, *Rsc Advances*, 7 (2017) 30894.
5. J. Ožbolt, G. Balabanić and M. Kušter, *Corrosion Science*, 53 (2011) 4166.
6. C.Q. Li, R.I. Mackie and W. Lawanwisut, *Computer-Aided Civil and Infrastructure Engineering*, 22 (2010) 335.
7. L. Fu, Y. Zheng, A. Wang, W. Cai, B. Deng and Z. Zhang, *Arab J Sci Eng*, 41 (2016) 135.
8. L. Fu, Y. Zheng, Q. Ren, A. Wang and B. Deng, *Journal of Ovonic Research*, 11 (2015) 21.
9. T.A. Østnor and H. Justnes, *Advances in Applied Ceramics*, 110 (2011) 131.
10. G. Jiang, M. Zhou, T.H. Chiu, X. Sun, J. Keller and P.L. Bond, *Environmental Science & Technology*, 50 (2016) 8084.
11. H.S. Wong, Y.X. Zhao, A.R. Karimi, N.R. Buenfeld and W.L. Jin, *Corrosion Science*, 52 (2010) 2469.
12. M. Nehdi, M.S. Alam and M.A. Youssef, *Engineering Structures*, 32 (2010) 2518.
13. E. Burger, J. Monnier, P. Berger, D. Neff, V. L'Hostis, S. Perrin and P. Dillmann, *Journal of Materials Research*, 26 (2011) 3107.
14. C.Q. Li and R.E. Melchers, *Magazine of Concrete Research*, 58 (2015) 567.
15. F. Han, H. Li, J. Yang, X. Cai and L. Fu, *Physica. E*, 77 (2016) 122.
16. A. Wang, L. Fu, T. Rao, W. Cai, M.-F. Yuen and J. Zhong, *Optical Materials*, 42 (2015) 548.
17. A. Wang, H.P. Ng, Y. Xu, Y. Li, Y. Zheng, J. Yu, F. Han, F. Peng and L. Fu, *Journal of Nanomaterials*, 2014 (2014) 3.
18. L. He, L. Fu and Y. Tang, *Catalysis Science & Technology*, 5 (2015) 1115.
19. T. Fatima, *Journal of Engineering Mathematics*, 69 (2011) 261.
20. M. O'Reilly, D. Darwin, J. Browning, L. Xing, C.E.L. Jr and Y.P. Virmani, *Aci Materials Journal*, 110 (2013) 577.
21. S.P. Palanisamy, G. Maheswaran, C. Kamal and G. Venkatesh, *Research on Chemical Intermediates*, 42 (2016) 1.
22. A. Wang, C. Wang, L. Fu, W. Wong-Ng and Y. Lan, *Nano-Micro Letters*, 9 (2017) 47.

23. L. Fu, T. Wang, J. Yu, W. Dai, H. Sun, Z. Liu, R. Sun, N. Jiang, A. Yu and C.-T. Lin, *2D Materials*, 4 (2017) 025047.
24. A. Królikowski and J. Kuziak, *Electrochimica Acta*, 56 (2011) 7845.
25. R.J. Yang, Y. Guo, F.M. Tang, X.P. Wang, R.G. Du and C.J. Lin, *Acta Physico-Chimica Sinica*, 28 (2012) 1923.
26. B.A. Miksic, M. Shen and J. Hicks, *Materials Performance*, 52 (2013) 48.
27. C. Xu, W.L. Jin, N. Huang, H.T. Wu, Z.Y. Li and J.H. Mao, *Magazine of Concrete Research*, 68 (2015) 1.
28. L.V. Žulj, M. Serdar, S. Martinez and D. Bjegović, *Addictive Behaviors*, 22 (2013) 655.
29. Z.H. Dong, S. Wei, A.Z. Guo and P.G. Xing, *Corrosion Science*, 56 (2011) 5890.
30. X. Shi, Y. Liu, M. Mooney, M. Berry, B. Hubbard and T.A. Nguyen, *Corrosion Reviews*, 28 (2011) 105.
31. L. Fu, A. Wang, F. Lyv, G. Lai, H. Zhang, J. Yu, C.-T. Lin, A. Yu and W. Su, *Bioelectrochemistry*, 121 (2018) 7.
32. L. Fu, A. Wang, G. Lai, C.-T. Lin, J. Yu, A. Yu, Z. Liu, K. Xie and W. Su, *Microchim. Acta.*, 185 (2018) 87.
33. I. Ray, G.C. Parish, J.F. Davalos and A. Chen, *Journal of Aerospace Engineering*, 24 (2010) 227.
34. Z.H. Dong, T. Zhu, W. Shi and X.P. Guo, *Acta Physico-Chimica Sinica*, 27 (2011) 905.
35. E.J. Akpan, J.E. Okokon and I.C. Etuk, *Asian Pacific Journal of Tropical Disease*, 2 (2012) 36.
36. A.S. Basse, J.E. Okokon, E.I. Etim, F.U. Umoh and E. Basse, *Indian Journal of Pharmacology*, 41,6(2010-02-12), 41 (2010) 258.
37. A.S. Okoli and C.U. Iroegbu, *Journal of Ethnopharmacology*, 92 (2004) 135.
38. A.K. Satapathy, G. Gunasekaran, S.C. Sahoo, K. Amit and P.V. Rodrigues, *Corrosion Science*, 51 (2009) 2848.
39. L.A. Nnanna, I.O. Owate, O.C. Nwadiuko, N.D. Ekekwe and W.J. Oji, *Philosophical Transactions of the Royal Society A Mathematical Physical & Engineering Sciences*, 337 (2013) 237.
40. P.C. Okafor, M.E. Ikpi, I.E. Uwah, E.E. Ebenso, U.J. Ekpe and S.A. Umoren, *Corrosion Science*, 50 (2008) 2310.
41. P. Banerjee, M. Satapathy, A. Mukhopahayay and P. Das, *Bioresources and Bioprocessing*, 1 (2014) 3.
42. S. Ahmed, Saifullah, M. Ahmad, B.L. Swami and S. Ikram, *Journal of Radiation Research and Applied Sciences*, 9 (2016) 1.
43. S.M. Pourmortazavi, M. Taghdiri, V. Makari and M. Rahimi-Nasrabadi, *Spectrochimica Acta Part A: Molecular and Biomolecular Spectroscopy*, 136 (2015) 1249.
44. M. Prabakaran, S.-H. Kim, V. Hemapriya and I.-M. Chung, *Journal of Industrial and Engineering Chemistry*, 37 (2016) 47.
45. A. Singh, I. Ahamad and M.A. Quraishi, *Arabian Journal of Chemistry*, 9 (2016) S1584.
46. M. Deyab, *Desalination*, 384 (2016) 60.
47. D. Bouknana, B. Hammouti, M. Messali, A. Aouniti and M. Sbaa, *Asian Pacific Journal of Tropical Disease*, 4 (2014) S963.
48. M. Lebrini, F. Robert and C. Roos, *Int. J. Electrochem. Sci.*, 6 (2011) 847.
49. L. Ruan, Z. Zhang, X. Huang, Y. Lyu, Y. Wen, W. Shang and L. Wu, *Int. J. Electrochem. Sci.*, 12 (2017) 103.
50. L. Guo, G. Ye, I.B. Obot, X. Li, X. Shen, W. Shi and X. Zheng, *Int. J. Electrochem. Sci.*, 12 (2017) 166.
51. N.A. Odewunmi, S.A. Umoren and Z.M. Gasem, *Journal of Environmental Chemical Engineering*, 3 (2015) 286.
52. X. Li, S. Deng and H. Fu, *Corrosion Science*, 62 (2012) 163.
53. B. Abd-El-Nabey, A. Abdel-Gaber, M.E.S. Ali, E. Khamis and S. El-Housseiny, *Int J Electrochem Sci*, 8 (2013) 5851.

54. M. Chevalier, F. Robert, N. Amusant, M. Traisnel, C. Roos and M. Lebrini, *Electrochimica Acta*, 131 (2014) 96.
55. M. Dahmani, A. Et-Touhami, S. Al-Deyab, B. Hammouti and A. Bouyanzer, *Int. J. Electrochem. Sci.*, 5 (2010) 1060.
56. F. Suedile, F. Robert, C. Roos and M. Lebrini, *Electrochimica Acta*, 133 (2014) 631.
57. M. Lebrini, F. Robert and C. Roos, *Int. J. Electrochem. Sc.*, 5 (2010) 1698.
58. M. Lebrini, F. Robert, P. Blandinières and C. Roos, *Int. J. Electrochem. Sci.*, 6 (2011) 2443.
59. M. Lebrini, F. Robert, A. Lecante and C. Roos, *Corrosion Science*, 53 (2011) 687.
60. G. Ji, S.K. Shukla, P. Dwivedi, S. Sundaram and R. Prakash, *Ind. Eng. Chem. Res.*, 50 (2011) 11954

© 2018 The Authors. Published by ESG (www.electrochemsci.org). This article is an open access article distributed under the terms and conditions of the Creative Commons Attribution license (<http://creativecommons.org/licenses/by/4.0/>).